



Article

Activating Transcription Factor 1 (ATF1) Immunohistochemical Marker Distinguishes HCCC from MEC

Wafaey Badawy¹, Asmaa S. Abdelfattah^{2,*} and Haneen A. Sallam³

¹ Department of Pathology, Alkharj (AKMICH), Military Industries Hospital, Kingdom of Saudi Arabia (KSA), Al-Kharj 16274, Saudi Arabia

² Faculty of Dentistry, Cairo University, Giza 12613, Egypt

³ Faculty of Dentistry, Horus University in Egypt, New Damietta 5006401, Egypt

* Correspondence: asmaaabdelfattah@dentistry.cu.edu.eg

Abstract: The study aimed to compare 15 cases of mucoepidermoid carcinoma (MEC) and 15 cases of hyalinizing clear cell carcinoma (HCCC) using immunohistochemical staining and molecular analysis. Thirty samples were examined, and markers, including p63, CK5/6, SOX10, CK7, ATF1, and FISH probes specific to *EWSR1* and *MAML2*, were used. Clear cell differentiation was observed in all MEC cases to some extent, with clear cell MEC showing the most prominent findings. Clear cell features were also present in conventional MEC, oncocytic MEC, and Warthin-like MEC, although to a lesser extent. The majority of cases were classified as low-grade MECs. *MAML2* rearrangement was detected in all cases (except cases 11 and 14), while *EWSR1* rearrangement was observed in a single case of clear cell MEC. These findings helped identify distinct subtypes within the mucoepidermoid carcinoma spectrum. The study emphasized the importance of utilizing immunohistochemical profiles, histopathological features, and molecular analysis for accurate diagnosis and classification of salivary gland neoplasms. HCCC was also discussed, and ATF1 was proposed as a marker to distinguish HCCC from morphologically similar neoplasms. The study concluded that a comprehensive approach combining immunohistochemistry, histopathology, and clinical correlation is essential for accurate diagnosis and classification, considering the variable expression of markers and potential overlap with other tumor types.

Keywords: hyalinizing clear cell carcinoma; mucoepidermoid carcinoma; *EWSR1*; *MAML2*; ATF1



Citation: Badawy, W.; Abdelfattah, A.S.; Sallam, H.A. Activating Transcription Factor 1 (ATF1) Immunohistochemical Marker Distinguishes HCCC from MEC. *J. Mol. Pathol.* **2023**, *4*, 178–188. <https://doi.org/10.3390/jmp4030016>

Academic Editors: Bacem Khalele and Giancarlo Troncone

Received: 29 May 2023

Revised: 16 July 2023

Accepted: 28 July 2023

Published: 1 August 2023



Copyright: © 2023 by the authors. Licensee MDPI, Basel, Switzerland. This article is an open access article distributed under the terms and conditions of the Creative Commons Attribution (CC BY) license (<https://creativecommons.org/licenses/by/4.0/>).

1. Introduction

HCCC was initially described as a distinct entity characterized by prominent stromal hyalinization. However, the 2017 WHO classification of head and neck tumors adopted the term clear cell carcinoma (CCC) and included HCCC as a synonym. This change emphasized the common molecular alterations (*EWSR1* rearrangement) shared by CCCs with or without hyalinization [1]. The classification debate revolves around whether HCCC should be considered a separate subtype or simply a morphological variant of CCC. HCCC has been associated with the potential for transformation into high-grade tumors. This association is supported by molecular studies demonstrating the presence of the same *EWSR1* rearrangement in both conventional and high-grade cellular components of the neoplasms [2,3]. Although HCCC is typically associated with a chromosomal translocation involving the *EWSR1* gene at 22q12.2, resulting in the fusion genes *EWSR1::ATF1* (*EWSR1* exon 8-*ATF1* exon 4, *EWSR1* exon 7-*ATF1* exon 4, and *EWSR1* exon 7-*ATF1* exon 5) or *EWSR1::CREM* [4,5], other fusions in a subset of HCCC may involve *EWSR1*-*PLAG1* or the *SMARCA2* and *CREM* genes between exon 4 of *SMARCA2* and exon 5 of *CREM* [6]. This suggests that HCCC represents a spectrum of differentiation rather than a separate neoplasm. The mechanism underlying this transformation and the factors influencing its occurrence are still unknown.

Immunohistochemistry (IHC) does not play a definitive role in the diagnosis of HCCC. Markers commonly used to diagnose HCCC include cytokeratin 5/6 (CK5/6), p63, p40, smooth muscle actin (SMA), S-100 protein, and calponin. Epithelial markers are used to confirm the epithelial nature of tumors and differentiate them from mesenchymal or lymphoid tumors [7], and they are helpful in diagnosing adenocarcinomas, mucoepidermoid carcinoma, and other epithelial malignancies. For example, CK7 is commonly expressed in mucoepidermoid carcinoma, while CK5/6 is seen in basaloid salivary gland tumors. CK19 is expressed in both benign and malignant salivary gland tumors, including adenoid cystic carcinoma and basal cell adenoma. Myoepithelial markers are important for distinguishing between myoepithelial-rich tumors and other salivary gland neoplasms because they can identify myoepithelial differentiation, such as pleomorphic adenoma, myoepithelioma, and adenoid cystic carcinoma. HCCCs typically show positivity for CK5/6, p63, and p40, while the myoepithelial markers (SMA, calponin) are usually negative. However, there can be variations in immunoreactivity, and IHC results are interpreted cautiously, considering the morphological context and other supporting findings. HCCCs must be distinguished from renal cell-like sinonasal adenocarcinoma, clear cell variant squamous cell carcinoma, and clear cell mucoepidermoid carcinoma [8].

This retrospective study investigated the expression of ATF1 in MEC and HCCC. Immunohistochemical staining for ATF1 was performed to evaluate its presence and intensity in both types of carcinomas after molecularly verifying that the cases met established inclusion criteria.

2. Materials and Methods

2.1. Cases Selections

We performed histologic examinations of 30 samples, out of which 15 were cases of MEC and 15 were HCCC. It is important to note that all of the cases of MEC exhibited clear cell differentiation to some degree. The most remarkable findings were observed in cases diagnosed as clear cell MEC. However, clear cell differentiation was also present, albeit to a lesser extent, in the cases of conventional MEC, oncocytic MEC, and Warthin-like MEC. The presence of clear cell features was a necessary inclusion criterion for comparing MECs to HCCCs, with cases of clear cell MEC being prominent in the selected samples. The ages of the included MEC and HCCC samples were comparable, with confounders discarded.

2.2. Eligibility Criteria

The inclusion criteria aimed to identify MEC cases with specific genetic rearrangements (*MAML2* positive, *EWSR1* negative) or distinct histopathological features, along with specific immunohistochemical marker expression (positive p63, negative SOX10). MEC cases meeting any of the following criteria were included: those positive for *MAML2* rearrangement and negative for *EWSR1* rearrangement; cases with three conspicuous neoplastic components; and cases showing positive p63 immunostaining and negative SOX10 immunostaining. Conversely, HCCC cases were excluded if they showed positive *MAML2* rearrangement or did not meet the specified criteria for *MAML2* negativity. These criteria ensured the selection of representative MEC cases with specific molecular and histopathological characteristics for comparison with *MAML2*-negative HCCC cases. The study aimed to investigate the differences between MEC and HCCC based on specific genetic and immunohistochemical markers. By implementing these well-defined inclusion and exclusion criteria, the study ensured the selection of appropriate cases for a meaningful and accurate comparison between MEC and HCCC, thus enhancing the reliability and validity of the findings.

2.3. Selection of Antibodies

All cases were stained with p63, CK5/6, SOX10, CK7, and ATF1. P63 is a transcription factor that is crucial for the development and maintenance of epithelial tissues. MEC and HCCC cases are always positive for p63. CK7 is a cytokeratin marker commonly expressed

in glandular and ductal epithelial cells. In MEC and HCCC, positive CK7 staining highlights the presence of luminal cells, aiding in the identification of the glandular component of the tumor. CK5/6 is a cytokeratin marker expressed by basal cells in various epithelial tissues. Positive CK5/6 staining further supports the diagnosis of MEC and HCCC and assists in distinguishing MEC and HCCC from other salivary gland tumors. SOX10 is a neural crest marker that is typically negative in MEC and HCCC. Its negative staining suggests the absence of neural crest differentiation and helps differentiate MEC and HCCC from other salivary gland tumors that may exhibit SOX10 positivity, such as adenoid cystic carcinoma and myoepithelial carcinoma. ATF1 is a transcription factor involved in cell growth and differentiation; prior to this study, it had not been tested in salivary gland neoplasms. Table 1 shows the product details of the used antibodies.

Table 1. Product details of the used antibodies.

Antibody	Mnf	Catalog no.	Clone	Staining Pattern	Dilution
ATF1	Abcam	ab47463	EPR4675	Nuclear	1:200
CK5/6	Dako	M7237	D5/16B4	Cytoplasmic	1:100
CK7	Dako	M7018	OV-TL 12/30	Membranous/Cytoplasmic	1:50
p63	Abcam	ab124762	4A4	Nuclear	1:100
SOX10	Abcam	ab155279	EP268	Nuclear	1:200

2.4. IHC Staining

For immunostaining, the paraffin-embedded tissue sections were first deparaffinized by immersing the slides in xylene or a xylene substitute. Subsequently, the sections were rehydrated using a series of graded alcohols, such as descending concentrations of ethanol or isopropanol, to prepare the tissue for antibody binding. Since paraffin fixation can mask antigens, antigen retrieval techniques were performed to unmask the antigen and enhance its accessibility for antibody binding.

For IHC preparation, heat-induced epitope retrieval was performed using a citrate buffer (pH 6.0). Following antigen retrieval, a commercially available protein-based blocking solution was used to block non-specific binding. The concentration of the blocking solution was prepared according to the manufacturer's instructions. After blocking, the primary antibody incubation step was carried out using an ATF1 monoclonal antibody. This involved applying the primary antibody which was then diluted at a concentration of 1:200 in an antibody diluent buffer. The slides were incubated overnight—at 4 °C or as recommended by the antibody datasheet to allow for optimal binding of the primary antibody to the target antigen. To remove all unbound primary antibodies and minimize background, the slides were washed three times for 5 min each using phosphate-buffered saline (PBS) with Tween 20 as the washing buffer. Subsequently, the slides underwent secondary antibody incubation, where an anti-mouse IgG conjugated with horseradish peroxidase (HRP) was used. The secondary antibody was diluted at a concentration of 1:500 in the antibody diluent buffer, and the slides were incubated for 1 h at room temperature. After the secondary antibody incubation, the slides were washed again using PBS. This washing step was performed three times for 5 min each. Following the washing steps, an enzymatic detection system, based on a commercially available HRP-based detection kit, was used according to the specific instructions provided by the manufacturer. Nuclear counterstaining was achieved using a counterstain, such as hematoxylin or DAPI. Finally, the slides were mounted with an aqueous mounting medium and subjected to digital image capture using a microscope equipped with a camera. Image analysis software, such as ImageJ or IHC, was utilized to set appropriate analysis parameters, including threshold and region of interest, for quantification of staining intensity or other desired parameters.

The staining intensity was evaluated by visually examining the stained tissue sections under a microscope. The intensity was typically described on a subjective scale, often

ranging from negative (no staining) to weak, moderate, and strong staining. We compared the staining intensity of the sample with known positive and negative controls to ensure consistency and accuracy in their interpretation. To ensure objectivity and minimize inter-observer variability, some studies employed digital image analysis software. In this study, the ImageJ IHC plugin was used to quantify the staining intensity based on color intensity or grayscale pixel values. It calculated the average intensity within specific regions of interest and generated numerical values or intensity scores for each sample. For histomorphologic analysis, thresholding was applied to convert the image into a binary image, separating stained regions from the background. This was typically achieved by selecting an appropriate threshold value that distinguished between stained and unstained areas based on color intensity. Regions of interest (ROIs) were manually or automatically selected to define specific areas of interest for quantification. These ROIs could encompass entire tissue sections or specific regions within the image. Once the ROIs were defined, ImageJ provided tools for measuring the staining intensity within those regions. The software calculated parameters such as integrated density, mean intensity, or area fraction occupied by stained pixels. The measured staining intensity values could then be further analyzed using statistical software or plotted to visualize differences between samples or experimental conditions. Background subtraction, color deconvolution, and co-localization analysis were not utilized in this study.

2.5. FISH Analysis

Paraffin blocks containing the tissue sections were first cut into 4-micrometer sections. The sections were then placed on charged microscope slides. The slides were immersed in xylene or a xylene substitute to remove the paraffin, which typically took several minutes. The deparaffinized slides were transferred to a series of graded alcohols, usually starting with 100% ethanol or isopropanol and gradually decreasing in concentration. This process helped rehydrate the tissue sections and remove any remaining traces of xylene or xylene substitute. The tissue sections underwent a pretreatment step to expose the target DNA sequences and improve probe accessibility. This step ensured that the slides were submerged in a retrieval buffer and subjected to a high temperature using a microwave or water bath. The exact conditions and duration of pretreatment varied depending on the specific FISH probe and protocol used.

Applying protease digestion aimed to enhance probe penetration and binding to the target DNA. The enzyme helped break down proteins and remove potential barriers that could hinder probe hybridization. The Zytovision FISH probe specific to *EWSR1* and *MAML2* detection was prepared according to the manufacturer's instructions. The probe was typically labeled with fluorescent markers or other detectable labels. The probe solution was applied to the tissue sections on the slides and covered with a coverslip. The slides were then placed in a hybridization oven or thermal cycler and incubated at a specific temperature for several hours to allow the probe to hybridize with the target DNA sequences in the tissue.

After the hybridization step, the slides were subjected to a series of post-hybridization washes to remove any unbound probe and reduce background signals. These washes typically involved immersing the slides in buffers of varying stringency and performing gentle agitation or shaking to facilitate the removal of excess probe. Excess liquid was removed, and the slides were allowed to dry in a dark environment overnight. The prepared slides were then visualized. An anti-fade mounting medium containing a DNA counterstain was applied to the slides to preserve the probe signals and provide contrast for visualization. Coverslips were placed on top of the slides, and the edges were sealed with an appropriate mounting medium. The prepared slides were examined using a fluorescence microscope equipped with appropriate filters to visualize the fluorescence signals emitted by the FISH probe. The *EWSR1* and *MAML2* translocation could be identified by the presence of a specific break apart rearrangement, indicative of the translocation event.

2.6. Statistical Analysis

The chi-square test is a suitable and valuable method for examining the relationship between the molecular expression patterns of *MAML2* and *EWSR1* rearrangements and the different carcinoma types (MEC and HCCC). This statistical test enables us to assess whether there is a significant association between these variables by analyzing the observed frequencies and their corresponding *p*-values.

3. Results

The presented cases demonstrated a diverse range of findings in mucoepidermoid carcinoma. The patients' ages ranged from 35 to 60, with a relatively equal distribution between males and females. Predominantly, the tumors were located in the parotid gland, although one case was observed in the sublingual gland and another in the palate. Immunohistochemical staining consistently revealed strong positivity for p63, CK5/6, CK7, and ATF1 in all cases, indicating their diagnostic relevance. Conversely, SOX10 staining was uniformly negative across all cases, suggesting the absence of neural crest differentiation or acinus formation. Furthermore, most cases were classified as low-grade mucoepidermoid carcinomas, underscoring the relatively favorable nature of these tumors. Molecular analysis revealed the presence of *MAML2* rearrangement in all cases, except cases 11 and 14. In contrast, no *EWSR1* rearrangement was observed in a single case of clear cell MEC. This case was not rediagnosed as adenocarcinoma, NOS, because dual fusions and double molecular hits are reported in non-hybrid salivary carcinomas.

These comprehensive immunohistochemical profiles and histologic features facilitated the identification of distinct subtypes within the mucoepidermoid carcinoma spectrum. The subtypes encompassed conventional, clear cell, oncocytic, Warthin-like, and mucinous variants, exemplifying the diverse nature of this neoplastic entity. These findings underscored the significance of incorporating molecular and histologic assessments for accurate classification and appropriate management of mucoepidermoid carcinoma cases, as shown in Table 2.

Table 2. Characteristics of the studied cases.

Case	Age	Sex	Site	p63	CK5/6	SOX10	CK7	ATF1	Grade	Stage	<i>MAML2</i> -Rearranged	<i>EWSR1</i> -Rearranged	Diagnosis
1	45	F	Parotid	++++	++++	-ve	++++	-	LG	II	Yes	No	Conventional MEC
2	52	M	Submandibular	++++	++++	-ve	++++	-	LG	III	Yes	No	Clear cell MEC
3	35	F	Parotid	++++	++++	-ve	++++	-	LG	II	Yes	No	Oncocytic MEC
4	60	M	Parotid	++++	++++	-ve	++++	-	LG	II	Yes	No	Warthin-like MEC
5	48	F	Parotid	++++	++++	-ve	++++	-	LG	II	Yes	Yes	Clear cell MEC
6	42	M	Parotid	++++	++++	-ve	++++	-	LG	III	Yes	No	Clear cell MEC
7	55	F	Sublingual	++++	++++	-ve	++++	-	IG	II	Yes	No	Clear cell MEC
8	50	M	Parotid	++++	++++	-ve	++++	-	LG	II	Yes	No	Mucinous MEC
9	38	F	Parotid	++++	++++	-ve	++++	-	LG	II	Yes	No	Conventional MEC
10	43	M	Palate	++++	++++	-ve	++++	-	LG	III	Yes	No	Clear cell MEC
11	47	F	Parotid	++++	++++	-ve	++++	-	HG	II	No	No	Clear cell MEC
12	55	M	Submandibular	++++	++++	-ve	++++	-	LG	II	Yes	No	Oncocytic MEC
13	57	F	Tongue	++++	++++	-ve	++++	-	LG	II	Yes	No	Warthin-like MEC
14	39	M	Sublingual	++++	++++	-ve	++++	-	HG	III	No	No	Conventional MEC
15	41	F	Parotid	++++	++++	-ve	++++	-	LG	II	Yes	No	Clear cell MEC
16	45	F	Parotid	++++	++++	-ve	++++	++++	LG	II	No	Yes	HCCC
17	52	M	Palate	++++	++++	-ve	++++	++++	LG	II	No	Yes	HCCC
18	35	F	Palate	++++	++++	-ve	++++	++++	LG	III	No	Yes	HCCC
19	60	F	Palate	++++	++++	-ve	++++	++++	LG	II	No	Yes	HCCC
20	48	F	Palate	++++	++++	-ve	++++	++++	LG	II	No	Yes	HCCC

Table 2. Cont.

Case	Age	Sex	Site	p63	CK5/6	SOX10	CK7	ATF1	Grade	Stage	MAML2-Rearranged	EWSR1-Rearranged	Diagnosis
21	42	F	Palate	++++	++++	-ve	++++	++++	LG	III	No	Yes	HCCC
22	55	F	Palate	++++	++++	-ve	++++	++++	LG	II	No	Yes	HCCC
23	50	M	Parotid	++++	++++	-ve	++++	++++	LG	II	No	Yes	HCCC
24	38	F	Parotid	++++	++++	-ve	++++	++++	LG	I	No	Yes	HCCC
25	43	M	Palate	++++	++++	-ve	++++	++++	LG	II	No	Yes	HCCC
26	54	M	Tongue	++++	++++	-ve	++++	++++	LG	III	No	Yes	HCCC
27	53	M	Palate	++++	++++	-ve	++++	++++	LG	II	No	Yes	HCCC
28	49	M	Parotid	++++	++++	-ve	++++	++++	LG	II	No	Yes	HCCC
29	43	F	Palate	++++	++++	-ve	++++	++++	LG	III	No	Yes	HCCC
30	47	F	Parotid	++++	++++	-ve	++++	++++	LG	II	No	Yes	HCCC

Abbreviations: "LG" low grade, "IG" intermediate grade, "++++": strongly positive, "-ve": negative

Conventional MEC was characterized by neoplastic squamous, mucinous, and intermediate components. The squamous component consisted of polygonal cells with eosinophilic cytoplasm and distinct cell borders, resembling squamous epithelial cells. The mucinous component comprised glandular structures filled with mucin-producing cells. The intermediate component consisted of cells with features between squamous and mucinous cells. These components varied in proportion within the tumor, leading to different histologic patterns. Clear cell MEC was characterized by the presence of clear cytoplasm within the tumor cells. The cytoplasm appeared optically clear due to the accumulation of glycogen or lipid droplets. This clear cell change was typically seen in the intermediate or mucus-secreting cells of MEC (Figure 1). Oncocytic MEC revealed a predominance of oncocytic cells within the tumor with granular eosinophilic cytoplasm. The oncocytic change involved both squamous and mucinous components of MEC. Warthin-like MEC exhibited histologic features reminiscent of Warthin tumor without abluminal oncocytic cells. The cystic spaces were filled with eosinophilic material resembling lymphoid stroma. These cystic spaces were surrounded by lymphoid tissue, with transition zones showing neoplastic and metaplastic squamoid and mucinous differentiation.

Mucinous MEC was displayed by the abundant presence of extracellular mucin within the tumor. The tumor cells formed glandular structures filled with mucin-producing cells. The mucin appeared as pale, eosinophilic material within the tumor stroma.

Hyalinizing clear cell carcinoma showed a nesting, cord-like, and trabecular arrangement. Ducts and small cysts could be observed. Squamous differentiation and mucocytes were commonly seen: sheets or nests of polygonal cells with clear cytoplasm and distinct cell borders. The cytoplasmic clearing was attributed to the presence of glycogen or other intracellular substances. The tumor cells exhibited nuclear atypia and a hyalinized stroma and fibrous septae separating the neoplastic fascicles. Although its name suggested the presence of clear cells, tumors consisting entirely of clear cells were rare, and some tumors lacked clear cells completely. Tongue HCCC displayed a pagetoid pattern of spread. The stroma varied from densely hyalinized, resembling a basement membrane to desmoplastic or fibrocellular. The juxtaposition of these two stroma types was largely characteristic of HCCC (Figure 2). Immunoreactivity of MEC and HCCC for ATF1 is shown in Figure 3.

The expression of ATF1 in HCCCs showed strong and diffuse nuclear immunostaining. Conversely, ATF1 was found to be negative in all MECs, including clear-cell MEC, further highlighting its potential diagnostic value in distinguishing between these different carcinoma types (Figure 3). The distinct expression pattern of ATF1 in HCCC suggests that ATF1 could serve as a valuable surrogate marker for diagnosing this specific carcinoma type and implies its significant involvement in the molecular mechanisms underlying this carcinoma. FISH rearrangement of *EWSR1* in HCCC is shown in Figure 4.

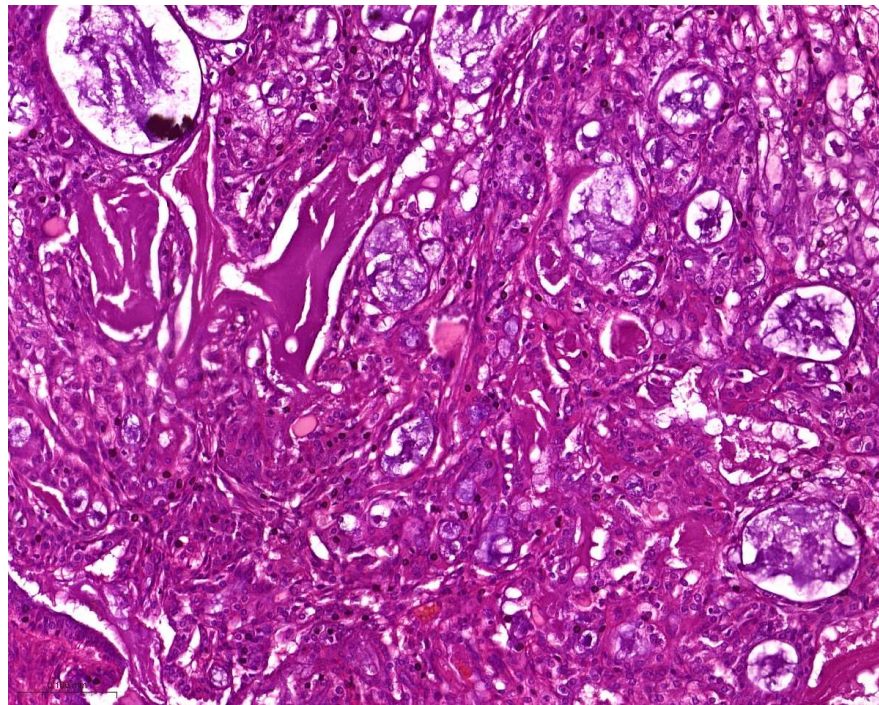


Figure 1. MEC with clear cell features. MEC architecture reveals a heterogeneous composition of mucin-secreting cells, epidermoid cells, and clear cells. Clear cells exhibit distinct transparent cytoplasm, lacking the typical granular or eosinophilic appearance seen in mucin-secreting and epidermoid cells. The nuclei of the clear cells are predominantly round or oval-shaped, exhibiting fine chromatin and prominent nucleoli. (H and E, magnification 20 \times).

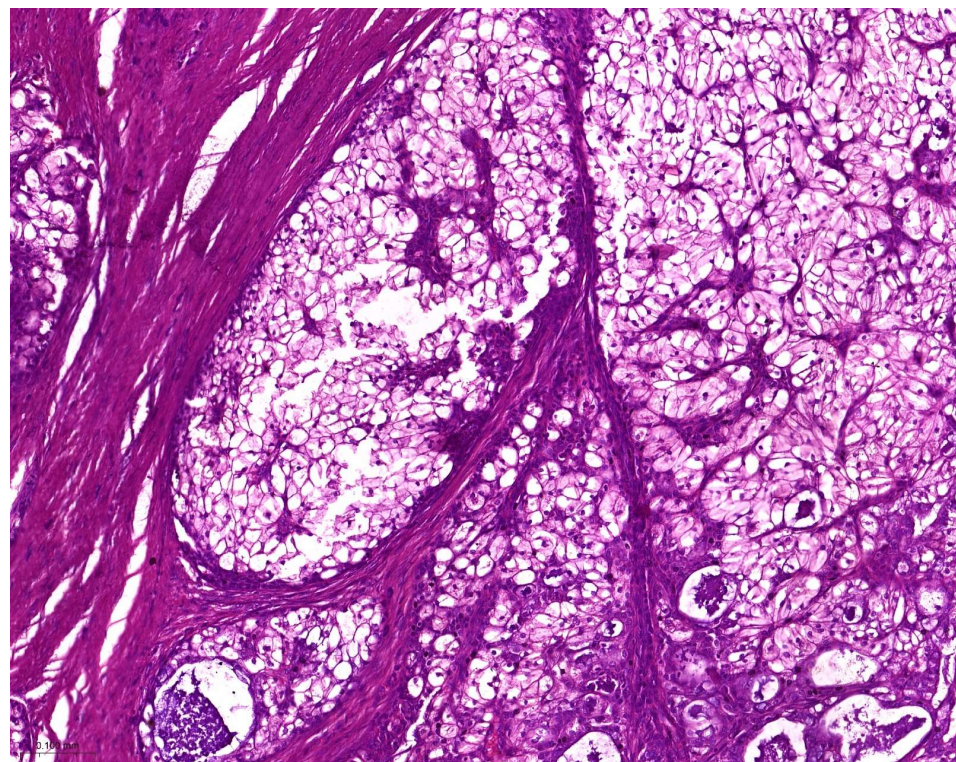


Figure 2. Hyalinizing clear cell carcinoma. The clear cells display a translucent cytoplasm, giving them a clear appearance, which is distinct from other cell types that have noticeable granularity or eosinophilia. Additionally, the tumor stroma contains hyaline-like material (H and E, magnification 20 \times).

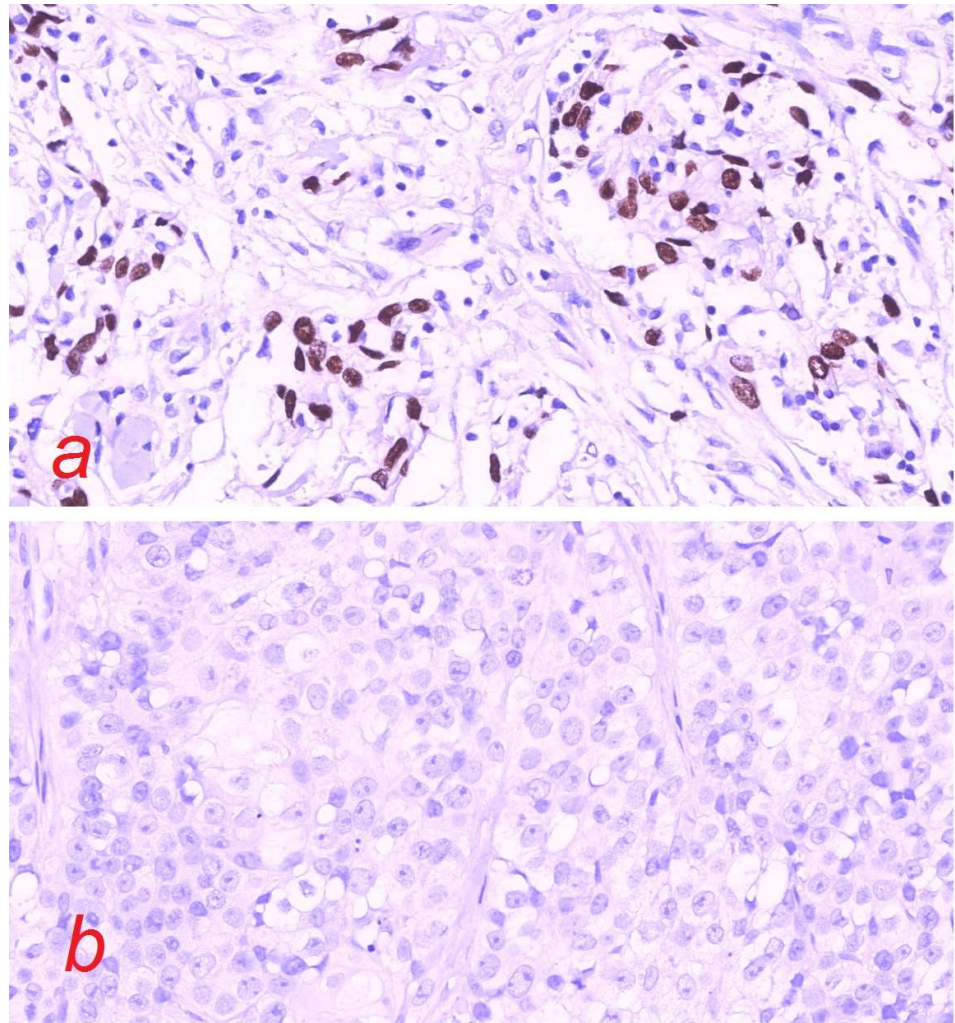


Figure 3. (a) ATF1-positive HCCC (magnification 40×), (b) ATF1-negative MEC (magnification 40×).

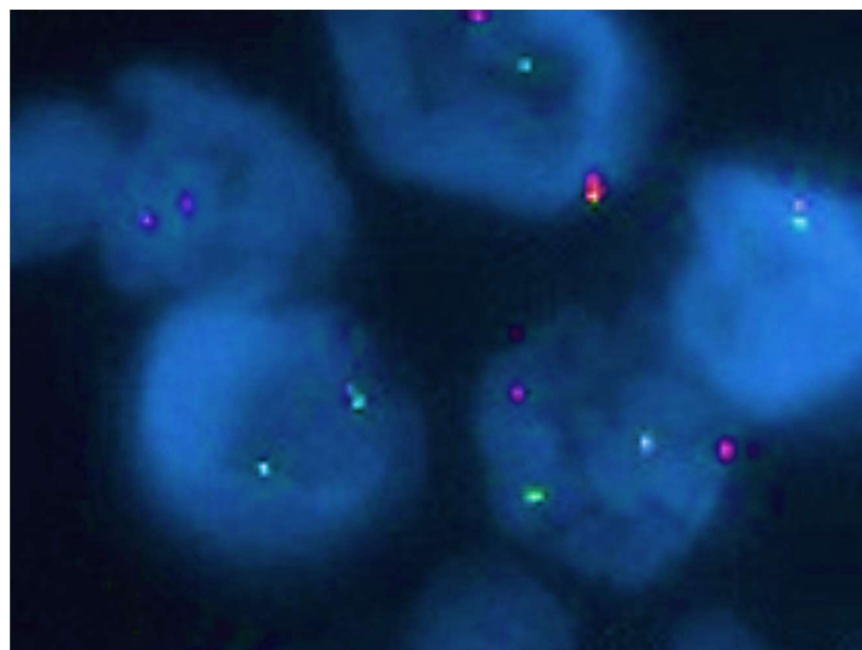


Figure 4. *EWSR1* rearrangement in HCCC.

A chi-square test was conducted to analyze the association between the rearrangement status (*MAML2* or *EWSR1*) and the group (MEC or HCCC). The test yielded a chi-square statistic of 27.0 with one degree of freedom, and the resulting *p*-value was 1.997×10^{-7} , indicating strong evidence against the null hypothesis. The small *p*-value ($p < 0.001$) suggests a significant association between the rearrangement status and the group. Therefore, we can conclude that there is a notable relationship between the molecular expression patterns of *MAML2* and *EWSR1* rearrangements and the different carcinoma types (MEC and HCCC).

4. Discussion

Salivary carcinomas are a heterogeneous group of tumors with few neoplasms that are molecularly labeled [9]. Acinic cell carcinoma is characterized by the presence of tumor cells with serous acinar cell differentiation for which the transcription factors NOR1 (also known as NR4A3) and Nurr1 (also known as NR4A2) have been identified as diagnostic markers, showing strong nuclear immunoreactivity [10–12]. Adenoid cystic carcinoma (AdCC) is a distinctive subtype characterized by its cribriform or tubular growth pattern. The MYB gene rearrangement has been identified as a specific genetic alteration in adenoid cystic carcinoma. Positive nuclear staining for MYB suggests adenoid cystic carcinoma [13,14]. Recently, protein kinase D1 (*PRKD1*) gene rearrangements have been identified as a recurrent genetic alteration in polymorphous adenocarcinoma [15–17] and cribriform adenocarcinoma of minor salivary glands [15,18,19]. Immunohistochemical staining for *PRKD1* can serve as a surrogate marker to support the diagnosis of one of these adenocarcinomas, if confused with AdCC.

HCCC is a rare epithelial malignant tumor of the salivary gland commonly occurring in the palate with an occasional predilection to occur in other sites of the oral cavity, characterized by *EWSR1::ATF1*, *EWSR1::CREM*, and *EWSR1::PLAG1* fusion scripts [20]. Pseudopapillae, i.e., gland-like spaces, and entrapped ducts were also observed in high-grade transformation cases. Testing for molecular fusion of *EWSR1::ATF1* is not always attainable in real-world practice. The specific oncogenetic mechanisms underlying the role of ATF1 in HCCC are yet to be elucidated. Nevertheless, it is believed that the dysregulated transcriptional activity of ATF1, resulting from gene rearrangements, leads to the abnormal expression of genes involved in CREB phosphorylation, TGF-beta signaling pathways, and survival pathways. This, in turn, contributes to the development and progression of salivary gland tumors.

Therefore, we tested 15 cases of HCCCs and 15 cases of MECs for ATF1 expression after molecular testing. Exploring ATF1 expression in cancer is a significant area of research, and the exercise of selecting, comparing, and discussing its most relevant findings can provide valuable insights into its potential role in tumorigenesis. ATF1, a transcription factor of the ATF/cyclic AMP response element-binding protein (CREB) family, has been implicated in various cancer types and is known to regulate multiple cellular processes involved in cancer progression. One of the relevant findings in ATF1 expression is its association with tumor aggressiveness and poor prognosis. ATF1 has been shown to enhance cell growth by promoting cell cycle progression and inhibiting apoptosis. Its overexpression has been observed in multiple cancer cell lines and tumor tissues, indicating a potential oncogenic role.

Although immunonegativity for ATF1 IHC marker does not rule out HCCC as the corresponding genes is detected in 73% of HCCCs, immunopositivity represents strong diagnostic evidence, which excludes the need for molecular testing. The practical advantages of using IHC surrogate markers include cost-effectiveness, ease of implementation, availability of antibodies, and compatibility with routine clinical practice. These advantages make IHC a valuable tool for assessing biomarker expression and supporting diagnostic and therapeutic decision making in various clinical settings. IHC techniques have been well established and standardized, allowing straightforward implementation into routine laboratory workflows [21]. Many laboratories are already equipped and staffed with per-

sonnel experienced in performing IHC staining, which further simplifies the process. Ease of implementation ensures that IHC surrogate markers can be readily incorporated into the diagnostic repertoire of pathologists and clinicians. More importantly, IHC staining can be performed on routine formalin-fixed, paraffin-embedded tissue sections exposed to heating during processing. These tissues do not contain viable DNA for molecular testing. However, IHC testing is still achievable. This study was not performed on MEC or HCCC arising in a pre-existing lesion.

5. Conclusions

Each tumor type may have different clinical courses, treatment approaches, and prognoses. Therefore, reliable diagnostic methods and markers that can accurately differentiate between these two tumor types contribute to improved prognostic evaluation and management decisions for patients. Hyalinizing clear cell carcinoma (HCCC) has been debated and researched due to its unique characteristics and diagnostic challenges. The debate surrounding HCCC revolves around the rarity of it showing clear cells entirely. Therefore, confusion with MEC cases is unavoidable. This research stands out due to its focus on ATF1 as a potential diagnostic marker for differentiating between MEC and HCCC. Through the evaluation of ATF1 expression and subsequent molecular verification, the study provides valuable insights into the diagnostic significance of this marker in distinguishing between these two types of carcinomas. We propose that ATF1 can distinguish between these morphologically similar neoplasms. The surrogate markers, histopathological examination, and clinical correlation contribute to the accurate diagnosis and classification of salivary gland neoplasms. However, the interpretation of immunohistochemical stains should be completed in the context of the overall clinical and histopathological findings, as some markers may show variable expression in different tumor subtypes or overlap with other tumor types. Validated surrogate markers can be valuable tools in clinical practice, providing clinicians with useful information for diagnosis, treatment decisions, and prognosis assessment.

However, the sample size of the study is small, with only 15 cases each of MEC and HCCC. A larger sample size would have provided a more robust and representative analysis of the molecular and immunohistochemical characteristics of these carcinomas. The findings should be interpreted with caution, considering the limited number of cases included. Moreover, the study relied on immunohistochemical staining and molecular analysis techniques specific to the markers of interest. However, next-generation sequencing (NGS), a more comprehensive and high-throughput genetic analysis method, was not employed. NGS could have provided a broader view of the molecular alterations and define the fusion scripts. The absence of NGS data limits the depth of genetic analysis and may not capture all relevant genetic alterations that could contribute to the differentiation and classification of these carcinomas. Future studies incorporating NGS could provide a more comprehensive understanding of the molecular landscape and potentially identify additional markers or genetic alterations relevant to MEC and HCCC differentiation. Considering these limitations, further research with larger sample sizes and advanced genetic analysis techniques, such as NGS, is warranted to validate and expand upon the findings of this study.

Author Contributions: W.B. is the lead author; A.S.A. and H.A.S. are supporting authors. All authors have read and agreed to the published version of the manuscript.

Funding: This research received no external funding.

Informed Consent Statement: Not applicable.

Data Availability Statement: Available upon reasonable request from the corresponding author.

Conflicts of Interest: The authors declare no conflict of interest.

References

1. Chapman, E.; Skalova, A.; Ptakova, N.; Martinek, P.; Goytain, A.; Tucker, T.; Xiong, W.; Leader, M.; Kudlow, B.A.; Haimes, J.D.; et al. Molecular profiling of hyalinizing clear cell carcinomas revealed a subset of tumors harboring a Novel EWSR1-CREM fusion: Report of 3 Cases. *Am. J. Surg. Pathol.* **2018**, *42*, 1182–1189. [[CrossRef](#)]
2. Jin, R.; Craddock, K.J.; Irish, J.C.; Perez-Ordóñez, B.; Weinreb, I. Recurrent Hyalinizing Clear Cell Carcinoma of the Base of Tongue with High-Grade Transformation and EWSR1 Gene Rearrangement by FISH. *Head Neck Pathol.* **2012**, *6*, 389–394. [[CrossRef](#)] [[PubMed](#)]
3. Skalova, A.; Leivo, I.; Hellquist, H.; Agaimy, A.; Simpson, R.H.W.; Stenman, G.; Vander Poorten, V.; Bishop, J.A.; Franchi, A.; Hernandez-Prera, J.C.; et al. High-grade Transformation/Dedifferentiation in Salivary Gland Carcinomas: Occurrence across Subtypes and Clinical Significance. *Adv. Anat. Pathol.* **2021**, *28*, 107–118. [[CrossRef](#)] [[PubMed](#)]
4. Solar, A.A.; Schmidt, B.L.; Jordan, R.C.K. Hyalinizing clear cell carcinoma: Case series and comprehensive review of the literature. *Cancer* **2009**, *115*, 75–83. [[CrossRef](#)]
5. Desai, A.; Rivera, C.M.; Faquin, W.C.; Iafrate, A.J.; Rivera, M.N.; Jaquinet, A.; Troulis, M.J. Clear cell carcinoma: A comprehensive literature review of 254 cases. *Int. J. Oral Maxillofac. Surg.* **2021**, *51*, 705–712. [[CrossRef](#)]
6. Lanic, M.D.; Guérin, R.; Sater, V.; Durdilly, P.; Ruminy, P.; Skálová, A.; Laé, M. A novel SMARCA2-CREM fusion expanding the molecular spectrum of salivary gland hyalinizing clear cell carcinoma beyond the FET genes. *Genes Chromosom. Cancer* **2023**, *62*, 231–236. [[CrossRef](#)]
7. Aljerian, K. EWSR1 rearrangement is not specific for hyalinizing clear cell carcinoma of salivary glands. *Ann. Diagn. Pathol.* **2022**, *59*, 151946. [[CrossRef](#)]
8. Luk, P.P.; Selinger, C.I.; Cooper, W.A.; Mahar, A.; Palme, C.E.; O’Toole, S.A.; Clark, J.R.; Gupta, R. Clinical Utility of In Situ Hybridization Assays in Head and Neck Neoplasms. *Head Neck Pathol.* **2019**, *13*, 397–414. [[CrossRef](#)]
9. Skálová, A.; Hyrcza, M.D.; Leivo, I. Update from the 5th Edition of the World Health Organization Classification of Head and Neck Tumors: Salivary Glands. *Head Neck Pathol.* **2022**, *16*, 40–53. [[CrossRef](#)] [[PubMed](#)]
10. Nguyen, L.; Chopra, S.; Laskar, D.B.; Rao, J.; Lieu, D.; Chung, F.; Kim, E.D.; de Peralta-Venturina, M.; Bose, S.; Balzer, B. NOR-1 distinguishes acinic cell carcinoma from its mimics on fine-needle aspiration biopsy specimens. *Hum. Pathol.* **2020**, *102*, 1–6. [[CrossRef](#)]
11. Freiberger, S.N.; Brada, M.; Fritz, C.; Höller, S.; Vogetseder, A.; Horcic, M.; Bihl, M.; Michal, M.; Lanzer, M.; Wartenberg, M.; et al. SalvGlandDx—A comprehensive salivary gland neoplasm specific next generation sequencing panel to facilitate diagnosis and identify therapeutic targets. *Neoplasia* **2021**, *23*, 473–487. [[CrossRef](#)] [[PubMed](#)]
12. Millan, N.; Tjendra, Y.; Zuo, Y.; Jorda, M.; Garcia-Buitrago, M.; Velez-Torres, J.M.; Gomez-Fernandez, C. Utility of NR4A3 on FNA cytology smears and liquid-based preparations of salivary gland. *Cancer Cytopathol.* **2022**, *130*, 949–954. [[CrossRef](#)]
13. Poling, J.S.; Yonescu, R.; Subhawong, A.P.; Sharma, R.; Argani, P.; Ning, Y.; Cimino-Mathews, A. MYB Labeling by Immunohistochemistry is More Sensitive and Specific for Breast Adenoid Cystic Carcinoma than MYB Labeling by FISH. *Am. J. Surg. Pathol.* **2017**, *41*, 973–979. [[CrossRef](#)] [[PubMed](#)]
14. Lee, J.H.; Kang, H.J.; Yoo, C.W.; Park, W.S.; Ryu, J.; Jung, Y.S.; Choi, S.W.; Park, J.Y.; Han, N. PLAG1, SOX10, and Myb expression in benign and malignant salivary gland neoplasms. *J. Pathol. Transl. Med.* **2019**, *53*, 23–30. [[CrossRef](#)] [[PubMed](#)]
15. Weinreb, I.; Zhang, L.; Tirunagari, L.M.S.; Sung, Y.S.; Chen, C.L.; Perez-Ordóñez, B.; Clarke, B.A.; Skalova, A.; Chiosea, S.I.; Seethala, R.R.; et al. Novel PRKD gene rearrangements and variant fusions in cribriform adenocarcinoma of salivary gland origin. *Genes Chromosom. Cancer* **2014**, *53*, 845–856. [[CrossRef](#)] [[PubMed](#)]
16. Katabi, N.; Xu, B. Polymorphous Adenocarcinoma. *Surg. Pathol. Clin.* **2021**, *14*, 127–136. [[CrossRef](#)]
17. Skálová, A.; Stenman, G.; Simpson, R.H.W.; Hellquist, H.; Slouka, D.; Svoboda, T.; Bishop, J.A.; Hunt, J.L.; Nibu, K.-I.; Rinaldo, A.; et al. The role of molecular testing in the differential diagnosis of salivary gland carcinomas. *Am. J. Surg. Pathol.* **2018**, *42*, e11–e27. [[CrossRef](#)]
18. Michal, M.; Skálová, A.; Simpson, R.H.W.; Raslan, W.F.; Čuřík, R.; Leivo, I.; Mukenšnábl, P. Cribriform adenocarcinoma of the tongue: A hitherto unrecognized type of adenocarcinoma characteristically occurring in the tongue. *Histopathology* **1999**, *35*, 495–501. [[CrossRef](#)]
19. Cocek, A.; Hronková, K.; Voldánová, J.; Sach, J.; Skálová, A.; Ambrus, M.; Vránová, J.; Hahn, A. Cribriform adenocarcinoma of the base of the tongue and low-grade, polymorphic adenocarcinomas of the salivary glands. *Oncol. Lett.* **2011**, *2*, 135–138. [[CrossRef](#)]
20. Nojima, S.; Kohara, M.; Harada, H.; Kajikawa, H.; Hirose, K.; Nakatsuka, S.I.; Nakagawa, Y.; Oya, K.; Fukuda, Y.; Matsunaga, K.; et al. Clear Cell Carcinoma in the Oral Cavity with Three Novel Types of EWSR1-ATF1 Translocation: A Case Report. *Head Neck Pathol.* **2022**, *16*, 560–566. [[CrossRef](#)]
21. Kuo, Y.; Lewis, J.S.; Truong, T.; Yeh, Y.; Chernock, R.D.; Zhai, C.; Hang, J. Nuclear expression of AFF2 C-terminus is a sensitive and specific ancillary marker for DEK::AFF2 carcinoma of the sinonasal tract. *Mod. Pathol.* **2022**, *35*, 1587–1595. [[CrossRef](#)] [[PubMed](#)]

Disclaimer/Publisher’s Note: The statements, opinions and data contained in all publications are solely those of the individual author(s) and contributor(s) and not of MDPI and/or the editor(s). MDPI and/or the editor(s) disclaim responsibility for any injury to people or property resulting from any ideas, methods, instructions or products referred to in the content.